




RESEARCH ARTICLE

Spectroscopy integration to miniature bioreactors and large scale production bioreactors—Increasing current capabilities and model transfer

Ruth C. Rowland-Jones¹  | Alexander Graf²  | Angus Woodhams³ |
Paloma Diaz-Fernandez¹  | Steve Warr¹ | Robert Soeldner² | Gary Finka¹ |
Marek Hoehse²

¹Biopharm Process Research, Biopharm Product Development and Supply, GlaxoSmithKline R&D, Stevenage, UK

²Product Development, PAT Corporate Research, Bioprocessing, Sartorius Stedim Biotech GmbH, Goettingen, Germany

³Hardware Development, The Automation Partnership (Cambridge) Limited, Hertfordshire, UK

Correspondence

*Paloma Diaz-Fernandez, Biopharm Process Research, Biopharm Product Development and Supply, GlaxoSmithKline R&D, Stevenage, UK.
Email: paloma.x.diaz-fernandez@gsk.com

Abstract

Spectroscopy techniques are being implemented within the biopharmaceutical industry due to their non-destructive ability to measure multiple analytes simultaneously, however, minimal work has been applied focussing on their application at small scale. Miniature bioreactor systems are being applied across the industry for cell line development as they offer a high-throughput solution for screening and process optimization. The application of small volume, high-throughput, automated analyses to miniature bioreactors has the potential to significantly augment the type and quality of data from these systems and enhance alignment with large-scale bioreactors. Here, we present an evaluation of 1. a prototype that fully integrates spectroscopy to a miniature bioreactor system (ambr[®]15, Sartorius Stedim Biotech) enabling automated Raman spectra acquisition, 2. In 50 L single-use bioreactor bag (SUB) prototype with an integrated spectral window. OPLS models were developed demonstrating good accuracy for multiple analytes at both scales. Furthermore, the 50 L SUB prototype enabled on-line monitoring without the need for sterilization of the probe prior to use and minimal light interference was observed. We also demonstrate the ability to build robust models due to induced changes that are hard and costly to perform at large scale and the potential of transferring these models across the scales. The implementation of this technology enables integration of spectroscopy at the small scale for better process understanding and generation of robust models over a large design space while facilitating model transfer throughout the scales enabling continuity throughout process development and utilization and transfer of ever-increasing data generation from development to manufacturing.

KEYWORDS

CHO cell culture, design of experiments (DOE), multivariate data analysis (MVDA), process analytical technologies (PAT), raman spectroscopy

1 | INTRODUCTION

The biopharmaceutical industry is ever increasing with its value in 2018 estimated at USD 237,250.8 million and predicted to increase to USD 388,997.3 million by 2024.¹ Therapeutic proteins offer improved specificity and highly potent and effective treatments for a wide variety of conditions many of which are chronic with significant impacts on quality of life and life expectancy² and also for emerging novel life-threatening human pathogens such as COVID-19.³

One key challenge in biopharmaceutical development is the numerous stages of development required for progressing a therapeutic protein⁴, with a key area being cell line development and screening. To aid in process development, there has been an uptake in the utilization of miniaturized high-throughput technologies, continuous data acquisition and data and knowledge driven tools for monitoring and control.⁵ Automated, high-throughput miniature bioreactors have been widely adopted in the industry to aid in automated screening of cell lines. These systems have many benefits such as being fully automated, can operate numerous bioreactors simultaneously, can mimic many of the characteristics of larger scale bioreactors, and can be used as scale-down models.^{6,7} However, at small scales (<15 ml), it can be challenging to operate them in a similar manner as large scale bioreactors due to the greater number of vessels to sample and reduced bioreactor working volume, limiting the number of offline measurements that can be taken. Furthermore, there has been a huge drive in the pharmaceutical industry to adopt process analytical technologies (PAT) as a result of the FDA PAT Initiative⁸ to enhance monitoring and control of processes. PAT, such as Raman⁹⁻¹¹ and NIR,¹² are being implemented for on-line monitoring in large scale vessels as they offer a non-destructive approach to measuring multiple analytes simultaneously. However, their use at small scale is limited due to the headspace requirements and capital costs associated with implementing for a large number of vessels. Work published in the literature demonstrates that techniques, such as Raman spectroscopy, have the potential to be applied as an at-line tool for measuring multiple analytes simultaneously using a 96 well plate format.¹³⁻¹⁵

A further key consideration for biopharmaceutical development is to be able to perform scale-up process characterizations in order to facilitate predicting performance at commercial manufacture scale from data generated at small scale.¹⁶ The use of similar analytical technologies and measurements across scales supports process characterization and scale-up. The transfer of spectral based models between scales has been considered in the literature. Strategies for calibration transfer have widely been discussed such as a calibration model developed for one instrument, which could be used to the required accuracy and precision for another instrument. Berry et al. (2015) sought to assess the scalability and transferability of PLS models developed using Raman spectra to predict multiple analytes across numerous scales.¹⁶ They demonstrated that accurate models for glucose, lactate, and osmolarity could be developed with various combination-scale calibration models however glutamate and ammonium models experienced limitations with single-scale calibrations. The smallest scale assessed was 5 L and all used an in-situ probe.

Webster et al. (2018) demonstrated the ability to transfer models built on 5 L scale data to a 10 L scale data for glucose, lactate, ammonium, viable cell concentration and total cell concentration, however models for product and glutamate were unable to accurately monitor changes.¹⁷ This was thought to be due to reference method errors and potentially could be addressed by ensuring better coverage of the full range of analyte concentration. In these examples, the same in-situ probes were used across scales. When transferring between ambr[®]15 scale and larger scale vessels there is the added challenge that the overall setup is different and identical probes between these scales are not currently available. The literature has shown that model transfer can be carried out from at-line laboratory to in-line industrial scale for liquid detergent compositions¹⁸ however; this required the use of standardization samples to be run in both experimental setups by gathering samples from the continuous manufacturing line and acquiring at-line Raman spectra, requiring additional sample measurements. This approach would however be very difficult to apply for biopharmaceuticals as media and inoculum will likely vary by batch lot, and seed train between the scales.

Here we present an integrated solution to a miniature bioreactor system (ambr[®]15) that not only enables fully automated setup for spectral acquisition but also facilitates model transfer across scales by using a spectral probe head with the same optical path despite varying sample presentation; an integrated setup to ambr[®]15 (static) through to on-line monitoring at 50 L scale (non-static) that can be applied to commercial scale vessels. The future era of Industry 4.0 envisions an intelligent data-driven manufacturing environment incorporating numerous advanced on-line analytics.¹⁹ The application of these tools across the scales will enable this vision to become a reality while leveraging large amounts of data generated in early development for commercial scale monitoring and control.

2 | METHODS

2.1 | Spectroscopy integration prototype

Prototypes of the Spectroscopy Platform (Sartorius Stedim Biotech) were used in this evaluation as integrated solutions for the ambr[®]15 and 50 L single-use bioreactor bag (SUB). A standard ambr[®]15 (Sartorius Stedim Biotech) was adapted to allow for integrated Raman measurements. Figure 1 displays the prototype setup, including data flow and spectrometer control. The liquid handling capabilities of an ambr[®]AM (analysis module) were extended by adding a prototype optical flow cell (1 mm path length, sapphire windows). The sample cup was connected to the entrance of the flow cell and the exit was connected to the waste bottle. A prototype optical probe head connected the flow cell and the Raman spectrometer (HyperFlux PRO PLUS, probe, and spectrometer, Tornado Spectral Systems). The ambr[®]15 control software was supplemented with a module to allow instrument control of the Raman spectrometer (start/stop measurement) and transfer of spectral data from the Raman instrument to the ambr[®]15 computer. This data was then merged with relevant

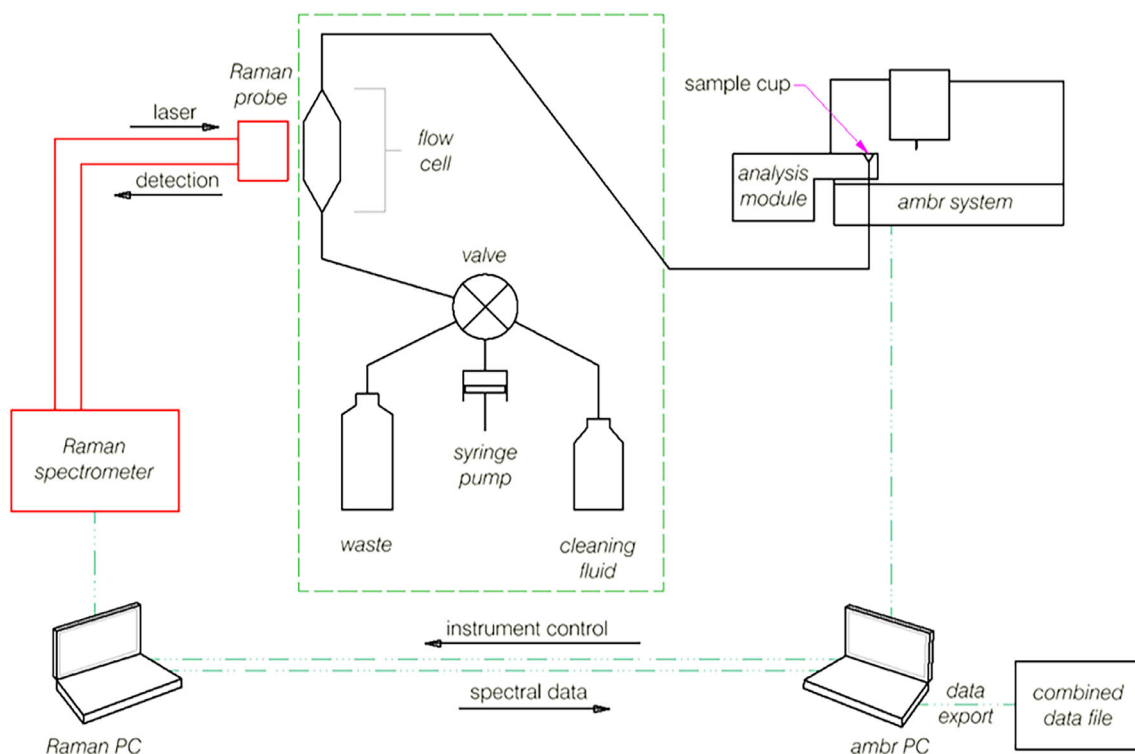


FIGURE 1 Schematic of the ambr®15 integrated spectroscopy solution prototype

bioreactor data (e.g., vessel number, ID, batch ID, sampling time, batch age, reference data) and jointly exported as a CSV file for model building.

A prototype of the 50 L SUB (Sartorius Stedim Biotech) was also evaluated. The Raman measurements in the large-scale SUBs required a measurement window and probe interface integrated into the bag film. Therefore, a prototype port containing sapphire windows was welded into the bag. The optical design of the port and spectral window material was comparable to the ambr®AM flow cell design therefore enabling the connection of a probe head same as that used for the ambr®15 integrated solution. The design of the SUB spectro port prototype prevents a direct light path between ambient light and detector, only light that scatters through the white polymer port has the chance of being detected. Therefore, the design is expected to have reduced sensitivity to ambient light. Raman instrument control was achieved using ambr®15 software on a separate computer.

2.2 | Cell culture

Four CHO-K1A derived cell lines (GSK) were used; two cell lines producing an IgG1 molecule (high and low producers relative to each other) and two cell lines producing an IgG2 molecule (high and low producers relative to each other).

The cell lines were revived in a proprietary chemically defined medium and maintained using GSK's proprietary cell culture conditions. The cell lines were passaged and scaled-up to generate a research cell bank (RCB) to be used for this work. For each production

run performed, a new vial of all four cell lines were revived from the RCB. This was carried out so that each production run was inoculated with cells of a similar generation number to minimize cell variation for a more objective comparison.

The GSK proprietary platform process was used for all production runs carried out. This was performed in fed-batch mode using glucose as the main carbon source that was controlled at a set point. Three supplementary nutrient feeds were added as bolus additions on days 0, 3, 6, 8, 10, and 14. The pH was controlled within the set points of the process using 1.5 M sodium carbonate and CO₂ additions. DO (dissolved oxygen) was controlled within the set points of the process by sparging with O₂ as necessary.

Three separate production runs were performed within ambr®15 miniature bioreactor systems (48 vessels/batches per system) using a working volume of 15 ml and four 50 L batches were carried out within SUBs. Both ambr®15 and 50 L scales were performed using the spectroscopy integrated solution setup as discussed previously.

The vessels within ambr®15 production run 1 were inoculated with the high producing cell lines and ambr®15 production run 2 vessels were inoculated with the lower producing cell lines. The ambr®15 production runs 1 and 2 aimed to provide data (both spectral and reference data) for model development to predict numerous analytes (discussed in more detail later). To enable this, a design of experiment (DOE) type approach was used to create in-vessel variation that spanned the design space of analyte concentrations of interest; glucose set point (3–7 g/L range) and seeding density ($1\text{--}1.4 \times 10^6$ cells/ml range). Further to this, additional spiking was performed outside of the vessel to break correlations between analytes for improved

subsequent model performance. This was achieved through the Spectroscopy ambr[®]15 software that has dedicated functionality for spiked samples that enabled sampling of each vessel, addition of spiking solution to the sample, sample aspiration in a well plate, take-up and delivery to the flow cell for spectral acquisition. Varying volumes of numerous stock solutions were added to a well plate to achieve a set concentration of spiked solution within the cell culture sample prior to spectral acquisition. Table 1 displays information on the stock solutions used for the spiking additions. Two stock solutions were used for each analyte (other than product). This was carried out to ensure changes observed were due to analyte addition and not to the dilution. Furthermore, two stock solutions were used to achieve a broad, equally distributed analyte range without falling below the minimal pipetting volume of the ambr[®]15 while keeping the sample dilution in an acceptable range.

Spectra were acquired on non-spiked and spiked samples on days 1, 2, 3, 6, 8, 10, 13, 15, 16, 17. Samples were also taken on these days and analysed for metabolite information. Cellular measurements were also obtained throughout the culture.

The third ambr[®]15 production run was used as a validation run. As a result, the system was inoculated with all four cell lines that were randomly assigned to the 48 vessels and the GSK proprietary platform process was applied. No in-vessel variation was performed, that is, process conditions and set points were applied and no spiking was performed outside of the vessel.

2.3 | Reference assays

Cell culture supernatant was analyzed using a Cedex HT Bio (Roche) to measure glucose, lactate, ammonium, glutamine, glutamate and product concentration in cell culture supernatant.

Cellular measurements were also obtained using an integrated Vi-Cell XR (Beckman) using the Trypan blue dye exclusion method.

2.4 | Spectroscopy

A Raman spectrometer (HyperFlux PRO PLUS, Tornado Spectral System) with a 785 nm laser was used. For both the ambr[®]15 and SUB

setup, the overall measurement time per sample was set to 5 min. To prevent detector saturation with increasing fluorescence over process time, single spectra exposure time, and averaging was adapted accordingly while still resulting in a total acquisition time of 5 min in all cases (e.g., 0.2 s × 300 accumulations × five spectra or 1 s × 60 accumulations × five spectra). The design of the ambr[®]15 measurement chamber, was optimized to block any directly incoming ambient light. The SUB spectro port was designed to minimize light interference as stated previously. A small shield of aluminium foil was used to protect the outside of the 50 L SUB port (however, the top of the bioreactor and the majority of the sensor windows were not covered). To account for any ambient light that strayed in the chamber or port, respectively, and therefore might reach the detector, a dark scan was performed. This was done prior to each sample measurement to account for potential variations in ambient light.

2.5 | Chemometric data analysis

Prior to analysis, the data was pre-treated. First, each spectrum was normalized to 1 s exposure time to account for the different exposure times due to varying fluorescence. The five spectra of each sample were then averaged to improve the signal-to-noise ratio. To correct for varying levels of fluorescence background, a number of different pre-processing techniques were assessed, including standard normal variate (SNV) followed by first derivative (Savitzky–Golay), however, asymmetric least squares smoothing (ALS) baseline correction algorithm²⁰ proved to be superior. All spectra were normalized to the integral of the water band at around 1,650 cm⁻¹ to correct for sensitivity differences between the various combinations of probes, fiber connections, and measurement chambers and spectrometer systems.

Raman spectra acquired were explored with the use of different multivariate data analysis (MVDA) tools. SIMCA version 16.0 (Sartorius Stedim Data Analytics AB) was used for all data analysis. Principal component analysis (PCA) was applied to explore variability within the datasets. Orthogonal-partial least squares (OPLS) regression was used to develop quantitative models for the different analytes of interest with the X-block dataset consisting of the spectral variables that were mean-centered while the Y-block was composed of the reference measurements that were UV-scaled (unit variance scaling). The spectral regions used for model building were selected according to those regions that were found to be unique for each analyte based on a DOE (discussed later).

Several criteria were utilized to determine optimal parameter settings for a robust, well-predicting model. The model should neither be under- nor overfitted, that is, that it fits the given data well and at the same time predicts datasets, that are not included in the model, with a similar error compared to the model error. In general, one aims for a high Goodness of Fit (R^2) while the goodness of prediction (Q^2) of the model increases as well. In the final model, the difference between R^2 and Q^2 should be below 0.2–0.3, otherwise, there is an indication that either some of the model components are unnecessary (over-fitting) or that some outliers are present that should be excluded.²¹ To obtain

TABLE 1 Stock solution information for spiking additions

Analyte	Stock solution (high) g/L	Stock solution (low) g/L
Glucose	32	8
Lactate	16	4
Glutamate	7	4
Glutamine	8	2
Ammonia	16	4
Product ^a	10.8	–

^aThis was only performed for the IgG1 molecule as no purified material was available to spike in IgG2.

a reliable Q^2 -value, the validation datasets were carefully selected. As one of the main goals of this work was the evaluation of the independency of the models with regard to cell line and molecule, four different CV-groups were assigned, each consisting of a single cell line / molecule combination. Four models were built (leave one cell line / molecule combination out) and evaluated separately thus mimicking four independent test set validations. Therefore, in all cases a cell line / molecule combination was predicted that was not in the calibration data set. The $RMSE_{CV}$ is the average error of the four built models as described above.

Other good indicators for the quality of OPLS models are the root mean square error of evaluation ($RMSE_E$) and the root mean square error of cross validation ($RMSE_{CV}$) where y_{cal} are the values predicted by the model or the cross-validation resampling strategy (y_{cvpred}) and y_i are the values from the reference method.

$$RMSE_E = \sqrt{\sum \frac{(y_i - y_{cal})^2}{N}}$$

$$RMSE_{CV} = \sqrt{\sum \frac{(y_i - y_{cvpred})^2}{N}}$$

Both $RMSE_E$ and $RMSE_{CV}$ values should be as low as possible. At the same time, the distance between them should also be low to avoid overfitting to the current dataset that may result in poor model performance when predicting future data sets.

Outliers were excluded using a number of methods. In the first step, the Score Plot of a PCA of the data was investigated. The spectra of points outside the Hotelling's T-square boundaries were further inspected. In case of apparent measurement failures (e.g., empty measurement chamber), the points were excluded. Single outliers present in the quantitative models, that is, in the observed versus predicted (CV) plots were also omitted after reconfirmation that they did not fit the data by their DModX-value. Overall, the outlier rate stayed below 2 %.

3 | RESULTS AND DISCUSSION

3.1 | Instrument setup

The experimental setup for the ambr[®]15 is shown in Figure 1. A measurement process of a standard bioreactor sample starts with the liquid handler sampling a bioreactor and release of the sample in the sample cup of the ambr[®]AM. The sample is transferred to the flow cell using a syringe pump. This is followed by the Raman measurement (785 nm excitation, 495 mW) and a cleaning cycle (standard washing liquid plus water) to prevent sample carry-over. Sample dilution by water residuals from the last water rinse of the cleaning cycle was determined to be around 1% (data not shown). For spiking samples, a known volume of a single analyte stock solution was added to a well plate. A bioreactor sample was then taken from a vessel using the

liquid handler and added to the stock solution sample. Both were mixed in the well plate by pipette aspiration and dispensing, followed by sample transfer to the sample cup and its delivery to the flow cell for measurement. SUBs were used at 50 L scale. The SUBs were designed to include an integrated spectral window comparable to the ambr[®]15 integrated solution, enabling the same Raman probe head as the ambr[®]15, to be attached externally. This resulted in on-line Raman acquisition without the requirement for an in-situ probe, removing the need for prior probe sterilization. The SUB port design yields reduced light interference as previously described.

3.2 | Experimental design

As discussed in the methods section, a DOE approach was used as well as spiking additions of stock solutions. This approach was used specifically to generate samples for model building to minimize correlations between analytes and maximize coverage of the design space.¹³ Cell cultivations are highly correlated processes with many analytes correlating with each other and/or with process time. Using a DOE approach resulted in differing process conditions and setpoint within the vessel leading to different process trajectories and reducing correlations. Furthermore, the DOE approach sought to build robustness into the model by ensuring greater variations than expected later in larger scale vessels – representing a broader design space so that all later cultivations fall within the limits.

The aim of the spiking additions was to further reduce the correlations¹⁶ and to increase the range of analytes measured. The range of analyte concentration is highly important for model building, especially with complex sample matrices such as cell culture, as the changes in the spectrum have to be significant to be able to link several intermediate concentrations to the spectral variations. As a "rule of thumb", a range of 10-fold in the reference/expected measurement should be included in the model.

3.3 | Spectral quality and clustering analysis

Three separate runs were performed in ambr[®]15 (each with 48 miniature bioreactors). The spectral quality was assessed during each complete run. During the course of the evaluation, data quality improved due to slight improvements with equipment setup, white light calibration and the running of the equipment. An OPLS model was developed to predict glucose concentration (model discussed in more detail later) that included all ambr[®]15 runs and the spiking data; scores plot displayed in Figure 2. The acquired Raman spectra of run 1 shows a large spread demonstrating variability. This is further demonstrated through systematic artefacts being observed in the contribution plot (data not shown) originating from insufficient white light calibration caused by variations of probe positioning between probe calibration and batch start. The hardware connection between flow cell and probe head was improved after the second run. Thus, the data quality improves by the third ambr[®]15 run demonstrated through the data

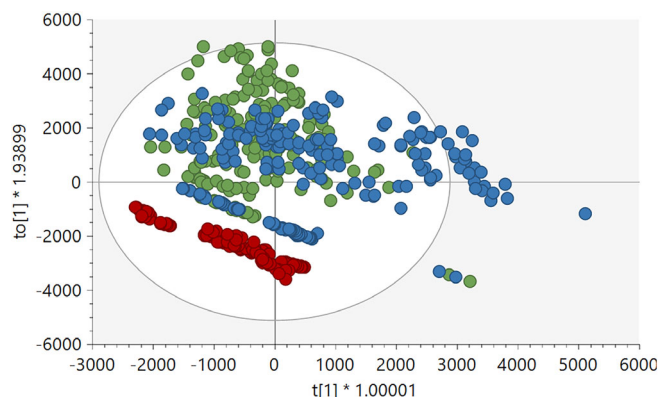


FIGURE 2 Scores plot of OPLS model developed to predict glucose concentration. Ambr[®]15 data; green: run 1, blue: run 2, red: run 3. OPLS, orthogonal-partial least squares

being clustered together in the scores plot (red) and the artefacts in contribution plot being smaller and did not show the sinus pattern as visible in the first batch (data not shown).

A PCA model was also developed focussing on the third ambr[®]15 run. During this run, all four cell lines producing two different molecules were cultivated in the normal GSK chemically defined process. Figure 3 displays the scores plot of the PCA model developed.

Cell lines denoted 1 and 2 produced the IgG2 molecule and cell lines denoted 3 and 4 produced the IgG1 molecule. The scores plots of the PCA model identifies natural clustering within the dataset. It can be observed overall, that the major source of clustering occurs with process trajectory; day 1 through to day 13. It is also demonstrated that there is generally good overlap of the four different cell lines (and therefore two different molecules) early in the process signifying that there is a high potential of developing good predictive

models generic for the molecule and cell line. From day 7, separation between cell lines occurs however, this is not due to the molecule as there is still good overlap as shown in Figure 3b. Further analysis identified that on the day of inoculation, cell line 1 (IgG2) and 4 (IgG1) were defined as lower producing cell lines and cell lines 2 (IgG2) and 3 (IgG1) were defined as higher producing cell lines. Separation is observed from days 7–10 based on this difference in productivity. Interestingly, however, cell line 1 (IgG2) demonstrated much lower productivity compared to the other three cell lines and this cell line appears to not follow the same trajectory in the scores plot as the other three cell lines (Figure 3a). This suggests that to develop a generic model for product concentration, it may be important to capture both good and bad performing cell lines in model development to ensure the model has been trained on all characteristics. This also shows the potential of using Raman spectra to identify unusual/differing performance between cell lines.

3.4 | Region selection

The spectral regions used for model building were pre-selected according to those regions that were found to be unique for each analyte, respectively. Figure 4 displays single analyte spectra (in water). As can be seen, unique peaks can be identified corresponding to glucose ($\sim 1,150\text{ cm}^{-1}$), lactate ($\sim 850\text{ cm}^{-1}$) and product (~ 900 and $1,000\text{ cm}^{-1}$). Peaks are observed for glutamine and glutamate however these have a weaker signal and those peaks that are visible are also present for other analytes indicating that they are not unique to those specific analytes. This suggests that it may be harder to develop specific models for glutamine and glutamate. Spectra were also obtained for ammonium in water however, no peaks can be seen. The literature suggests that model building may not be possible to directly measure ammonium concentration²² however, models have still been

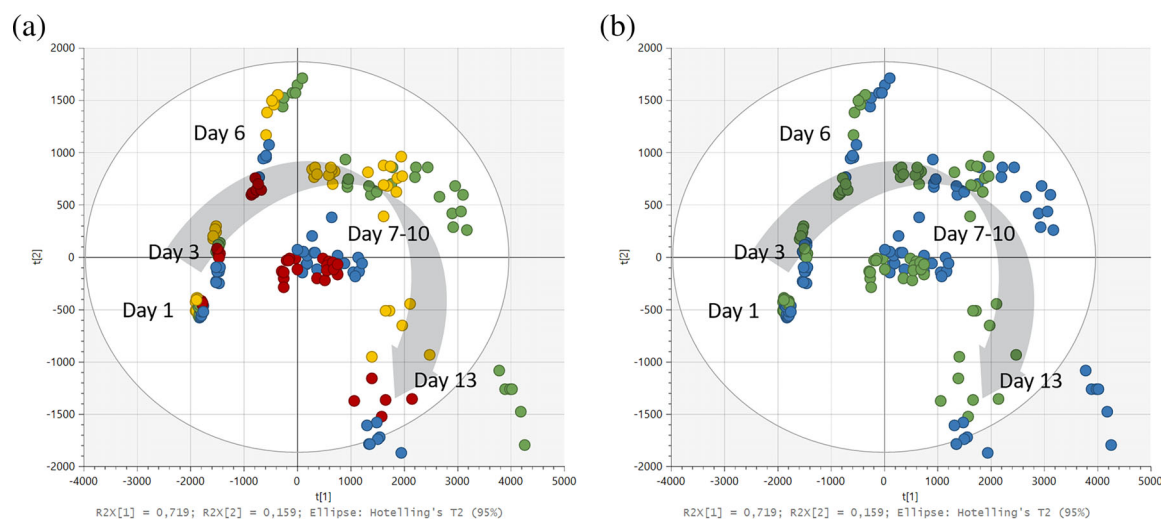


FIGURE 3 Scores plot of a PCA model developed on Raman acquired of ambr[®]15 run 3, (3 PCs, $N = 199$, $450\text{--}1800\text{ cm}^{-1}$). (a) coloured by cell line; green: cell line 1, blue: cell line 2, red: cell line 3, yellow: cell line 4., (b) coloured by molecule; green: IgG1, blue: IgG2. The arrows indicate the process trajectory. PCA, principal component analysis

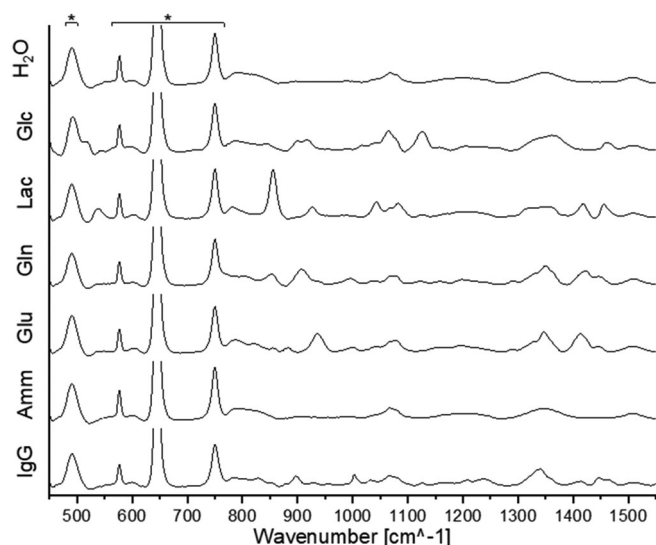


FIGURE 4 Single analyte spectra in water. *Sapphire bands from the integrated flow cell window

developed^{16,17,23} but these may be correlated with changes of other components in cell culture.

A DOE approach was applied to further study and identify Raman peaks that are unique for each analyte of interest. By using this approach, it also identifies which analytes can be directly measured using Raman spectroscopy and therefore models based on causality and those which are based on correlations. This approach also enables model performance in "optimum" conditions to be understood as the preparation of the samples was carried out under optimal laboratory conditions, with unchanging sample matrix without bubbles and particles, as well as using high accuracy balances to prepare the samples rather than relying on reference methods.

The study was designed with four concentration levels for each of the analytes glucose, lactate, glutamine, glutamic acid, ammonium, and BSA, respectively. In combination with three center-points, this resulted in 18 experiments. For the measurement, a re-usable probe (MarqMetrix) in combination with a Raman Spectrometer (HyperFlux PRO PLUS, Tornado Spectral Systems) was used. Each sample was measured in a glass vial, which was shielded from ambient light.

For the identification of unique peaks of each analyte, the collected spectra were first baseline corrected and then imported into SIMCA (Sartorius Stedim Data Analytics). OPLS models for each individual analyte were developed. For identifying unique wavenumbers, the variable importance in the projection (VIP) was utilized. The VIPs describe the influence of each x-variable – in this case, the wavenumbers – on the y-variable. The average of all VIPs always equals to one, and therefore variables with a VIP larger than one are assumed to be most important for describing y .²¹ By identifying the wavenumbers specific to each analyte, wavenumber regions specific for the analyte of interest could be included for model development, reducing potential correlations between analytes. The VIPs identified in this DOE study were later used for the model building with the ambr[®]15 and SUB data.

3.5 | Prediction of metabolites using orthogonal partial Least Square regression

Individual OPLS models were developed to correlate the Raman spectra with off-line measurements (Cedex) to produce predictive models for glucose, lactate, glutamine, glutamate and product concentration. Prior to model development, pre-processing was applied to the datasets and different regions of the spectra were included (discussed previously). Outlier identification was then carried out, initially using scores plots of PCA and then further by evaluating their Hotelling's T-square and DmodX-values (data not shown) and sum up to less than 2% of detected outliers. Figure 5 displays the observed versus predicted plots for each of the OPLS models developed.

OPLS models developed to predict lactate and glucose concentration demonstrated high accuracy sufficient for the application described in this study (0.28 g/L and 0.34 g/L RMSE_{CV} respectively). The model developed to measure product concentration also demonstrated good accuracy with an RMSE_{CV} of 0.22 g/L and all three models showed good correlation between the measured and predicted values (R^2 coefficient > 0.95). OPLS models were also developed to predict glutamine and glutamate however the errors, compared to the range in concentration observed, were high (0.038 g/L and 0.073 g/L RMSE_{CV} respectively) and the R^2 coefficient lower than the models for the other analytes (0.709 and 0.783 respectively). This is likely due to the low concentration of each analyte observed in cell culture and through non-specific analyte peaks observed in the spectra (discussed earlier). The models may be further improved through the addition of spectra of spiked cell culture (discussed later). A summary table of model performance is displayed in Table 2.

Raman spectra used for model development was acquired of four cell lines, two producing an IgG1 and two cell lines producing an IgG2 molecule. The models reported here demonstrate the ability to develop generic models that can be used for multiple cell lines and different molecules. This is aligned with other work published in the literature for on-line monitoring at larger scale.^{16,17}

An offline reference method was used for model calibration. As a result, there was a time delay between reference method and Raman spectra acquisition. This time difference can be up to several hours and may therefore result in differences in analyte concentrations that were measured offline and those later seen by the Raman spectrometer. To investigate the impact of this delay on model performance, the glucose concentration was approximated at the time of Raman sampling. For each spectrum at timepoint t_i , the glucose concentration was determined using a mass balance equation. First, the viable cell concentration (VCC) according to the Monod model for cell growth were calculated.²⁴

$$VCC_n = cX_0 \times e^{\frac{\ln cX_1 - \ln cX_0}{tX_1 - tX_0} (t_n - tX_0)}$$

The glucose concentration was calculated using the adjusted VCC at timepoint t_0 , t_1 and t_i , also taking into account that glucose-containing

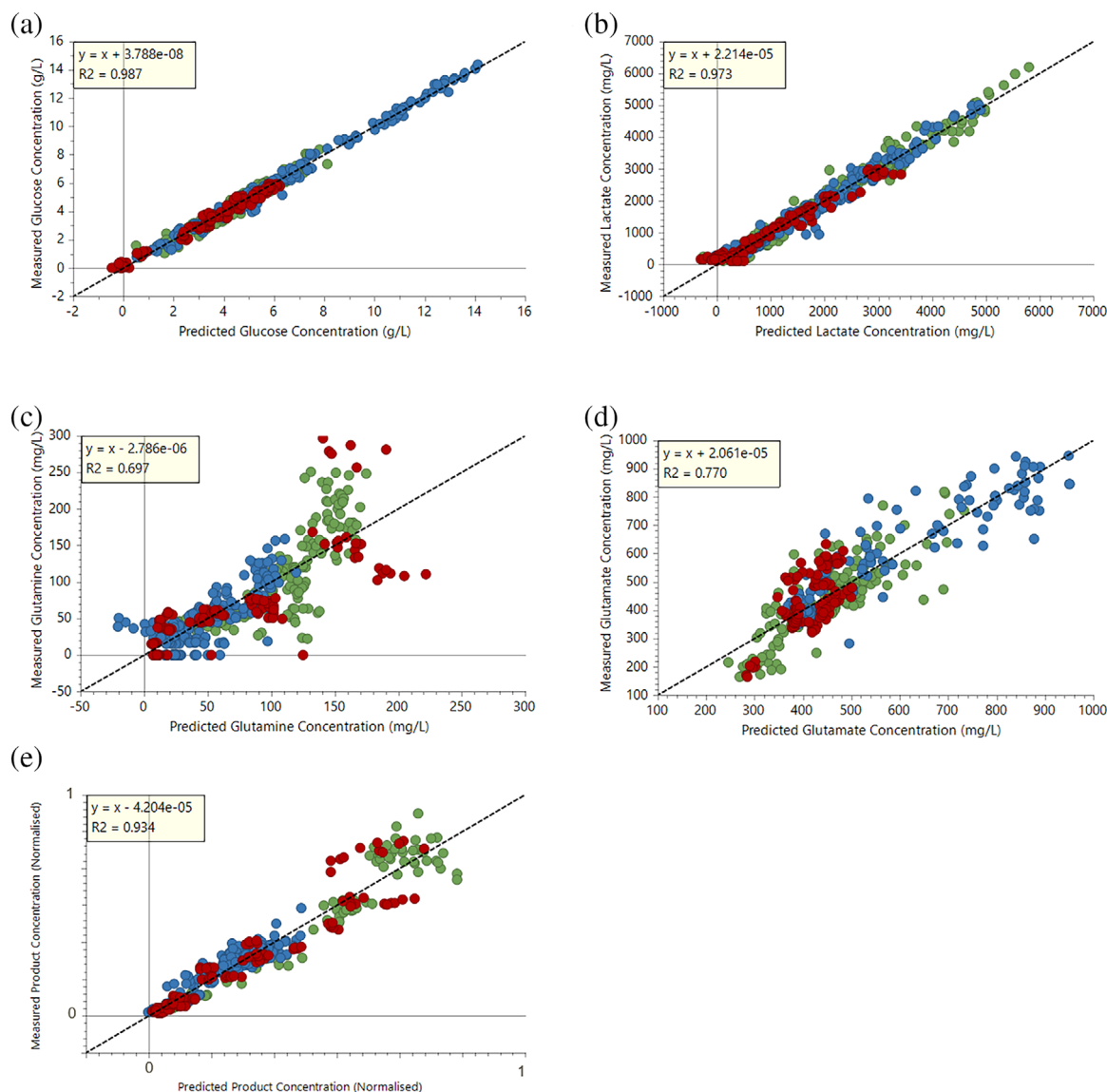


FIGURE 5 Observed versus predicted (cross-validation) plots for OPLS models developed to predict (a) glucose, (b) lactate, (c) glutamine, (d) glutamate, (e) product concentration. For all plots, green: ambr[®]15 run 1, blue: ambr[®]15 run 2, red: ambr[®]15 run 3. OPLS, orthogonal-partial least squares

TABLE 2 Summary of the final OPLS models developed with and without spiked samples

Analyte	Without spiked samples					With spiked samples				
	Range (g/L)	LV	R2	RMSE _C (g/L)	RMSE _{CV} (g/L)	Range (g/L)	LV	R2	RMSE _C (g/L)	RMSE _{CV} (g/L)
Glucose	0–14	1 + 4	0.987	0.31	0.37	0–18	1 + 4	0.984	0.35	0.40
Lactate	0–6	1 + 3	0.971	0.22	0.34	0–6	1 + 4	0.975	0.21	0.29
Glutamine	0–0.2	1 + 3	0.709	0.031	0.042	0–2.5	1 + 5	0.618	0.18	0.22
Glutamate	0.2–1	1 + 5	0.783	0.070	0.083	0–2	1 + 5	0.819	0.14	0.15
Product	Normalised	1 + 5	0.934	0.17	0.23	Normalised	1 + 6	0.923	0.20	0.37

Abbreviations: OPLS, orthogonal-partial least squares; RMSE_{CV}, root mean square error of cross validation.

feed medium was added and glucose was consumed by the cells at different rates over the course of a batch (fed-batch model)

$$VCC0 = VCCn(cX0, cX1, tX0, tX1, t0)$$

$$VCC1 = VCCn(cX0, cX1, tX0, tX1, t1)$$

$$VCCi = VCCn(cX0, cX1, tX0, tX1, ti)$$

$$q_s = \frac{(V0 \times cS0 + VF \times cSF - V1 \times cS1 - V_{\text{Sample}} \times cS0)}{(t1 - t0) \times \frac{VCC0 + VCC1}{2} \times \frac{V0 + V1}{2}}$$

cSi

$$= \frac{(V0 \times cS0 + VF \times cSF - u_{\text{rate}} \times VCCi \times (ti - t0) \times Vi - V_{\text{Sample}} \times cS0)}{Vi}$$

qS = average glucose consumption rate per cell between samples

cSi = calculated glucose concentration at timepoint ti

$cX0$ = VCC at timepoint $tX0$

$tX0$ = Closest timepoint before ti for vcc

$cX1$ = VCC at timepoint $tX1$

$tX1$ = Closest timepoint after ti for vcc

$t0$ = Closest timepoint before ti for specific measurement

$t1$ = Closest timepoint after ti for specific measurement

ti = Calculation timepoint

$V0$ = Volume at timepoint $t0$

$V1$ = Volume at timepoint $t1$

VF = Volume of added glucose feed

cSF = Glucose concentration within feed medium

$cS0$ = Glucose concentration at timepoint $t0$

$cS1$ = Glucose concentration at timepoint $t1$

V_{Sample} = Volume of taken sample

For automatization, these calculations were implemented in Python 3.7 with the Pandas 0.23.4 and numpy 1.15.4 library. For each batch, the corresponding files containing the above mentioned parameters were imported into the Python environment and after calculations the results were exported into a separate file. This new data

table was then imported into SIMCA along with the spectra for further evaluation. OPLS models were then developed to compare the use of the adjusted glucose offline values with the measured glucose values. OPLS models were developed to include only ambr[®]15 runs 2 and 3 (so as to use the better quality spectra as discussed earlier). Both models contained 1 + 3 principal components. Despite adjusting for the delay in measurement, the model using the measured value showed a smaller error ($RMSE_{CV} \sim 0.3$ g/L) compared to the model that used the adjusted glucose concentrations ($RMSE_{CV}$ 0.4 g/L); Figure 6. It is important to note, that the growth and feeding consumption kinetics for a mammalian process is slower compared to, for example, a bacterial process.^{25,26} This would also suggest that any delay in measurement may not significantly affect model performance. The difference in model performance is also likely due to additional errors incorporated through the complex calculations for adjusting the glucose concentration and measurement errors of the various input parameters. Therefore, for this example, more accurate models can be obtained through the use of the measured glucose concentration despite delays between the sample being taken, the offline reading and Raman spectral acquisition. Further improvement may be achieved through the use of an integrated reference method (assessment out of scope of the work presented here).

3.6 | Prediction of metabolites using orthogonal partial Least Square regression using spiked samples

One challenge of using spectroscopy techniques such as Raman for measuring multiple analytes in cell culture is that many of the components of interest are highly correlated. The literature has shown that more robust models can be generated by breaking these correlations, ensuring that the models developed are specific for the analyte and therefore influenced less by fluctuations in other components. This has been achieved through the use of DOE approaches¹³ and through spiking of known concentrations to deconvolute signal information.¹⁶ The ambr[®]15 spectroscopy integration solution has the ability to perform spiking additions of known volumes of a stock solution by

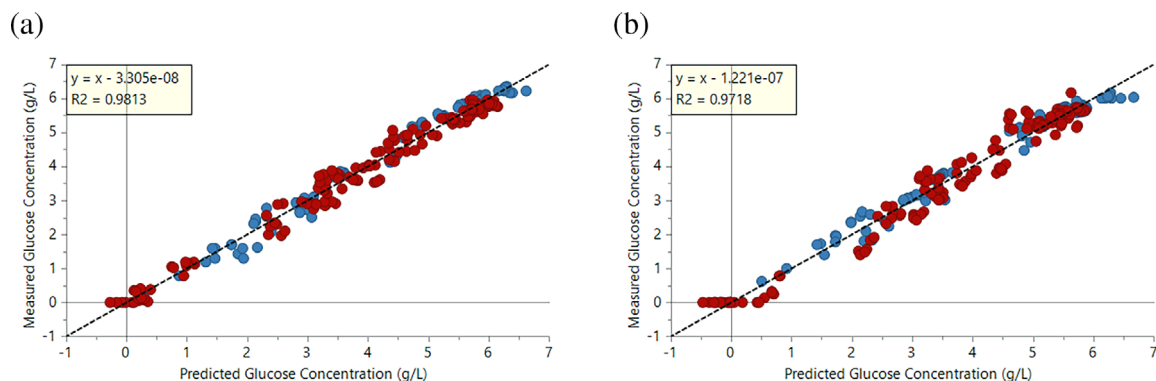


FIGURE 6 Observed versus predicted (cross-validation) plots for OPLS models developed using ambr[®]15 run 2 + ambr[®]15 run 3 using (a) measured glucose concentration, (b) adjusted glucose concentration. Blue: ambr[®]15 run 2. Red: ambr[®]15 run 3. OPLS, orthogonal-partial least squares

sampling from a vessel, delivering to a well plate (containing a known volume of stock solution), aspirating the sample and delivering it to the sample cup to be transferred through to the flow-cell for Raman spectra acquisition. This was performed to break correlations between analytes and to increase the range of concentration observed by the multivariate calibration model.

OPLS models were developed to include Raman spectra acquired of cell culture spiked with known volumes of a stock solution to vary the concentration of individual analytes. Pre-processing was applied to the spectra and outlier identification was carried out as discussed previously (data not shown). Figure 7 displays the observed versus predictive plots of the individual OPLS models developed correlating Raman spectra with glucose, lactate, glutamine, glutamate and product concentration.

As can be seen in Figure 7, the addition of the spiked samples increased the range in concentration for all analytes. This was less apparent for glucose and lactate concentration, which may result in reduced model performance when using these additional samples for model building. Table 2 displays the summary statistics of the models developed with and without the spiking samples.

Models including both spiked data (i.e., adding in a known volume of a stock solution to a sample prior to Raman acquisition) and non-spiked data were developed. Overall, the models demonstrate similar performance however, for those analytes at very low concentration; the spiking has resulted in a broader range to be explored. This is particularly important for models developed for glutamine and glutamate. For both these analytes, their concentration in the bioreactor samples are likely below the detection limit of the Raman instrument (~0.1–

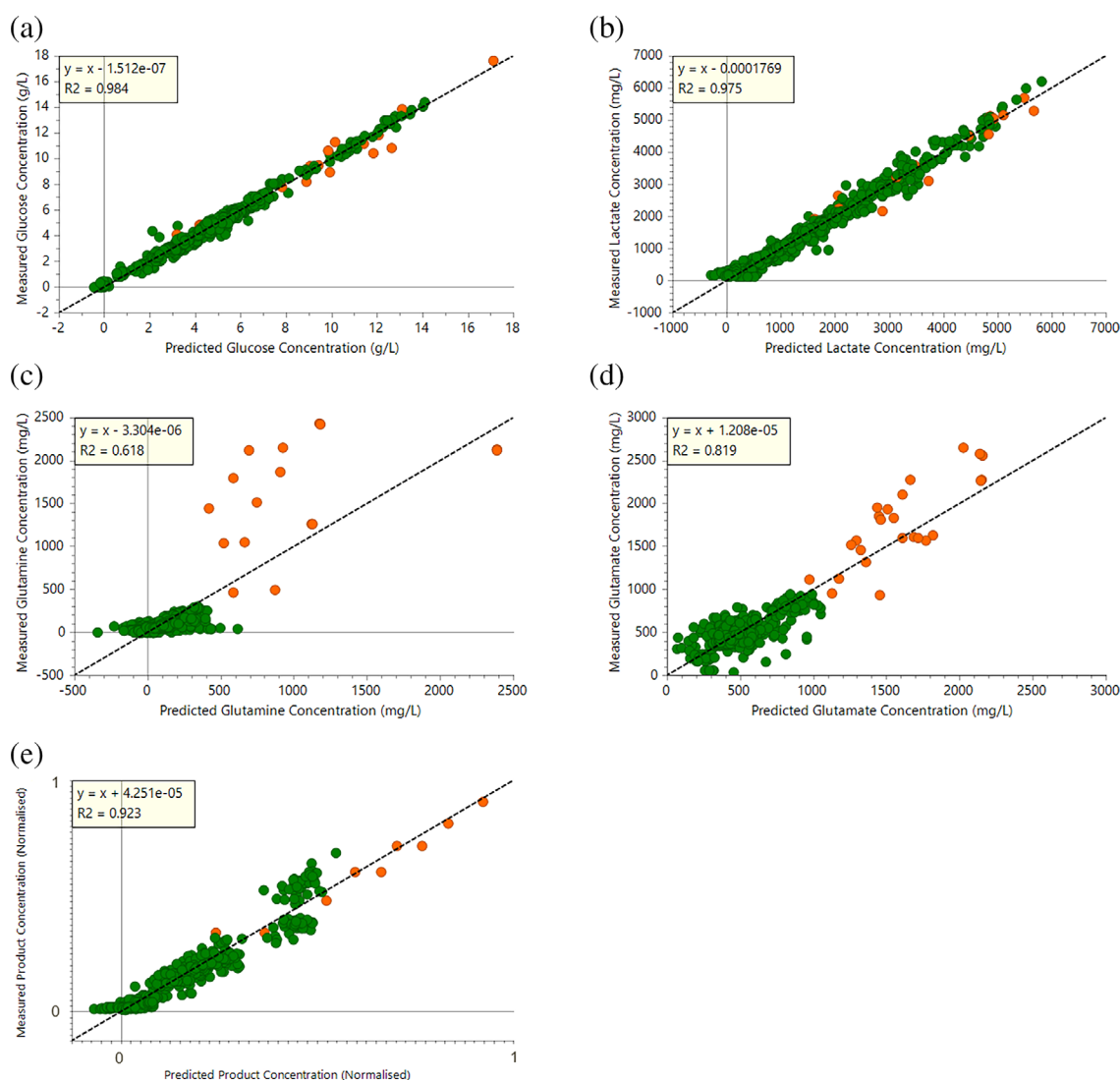


FIGURE 7 Observed versus predicted (cross-validation) plots of OPLS models developed for (a) glucose, (b) lactate, (c) glutamine, (d) glutamate, and (e) product concentration. For all plots, green: non-spiked samples, orange: spiked samples. OPLS, orthogonal-partial least squares

0.2 g/L). By including the spiking samples, the range is increased and enhances the likelihood of developing a causal model rather than one built on correlations.

An additional aim of using spiked samples was to break correlations between analytes ensuring model robustness to small fluctuations in cell culture samples. Table 3 and Table 4 display the correlation matrix of data without spiked samples and with spiked samples respectively. Values above 0.6 are considered to demonstrate a strong correlation for example, in Table 2 glutamine appears to be strongly correlated with product (0.886, Table 3), however, when introducing spiked samples, this correlation is reduced (0.08, Table 4). Product correlation to batch age was not completely broken (Table 3:0.739, Table 4:0.524). This is likely due to a smaller number of spiking samples generated for the model predicting product concentration. It is also important to note that there was only spiking material available for one product and therefore many vessel samples did not include product spiking. As a result, the time correlation is still present.

Overall, the correlation between the analytes is broken (or reduced) when introducing spiked samples. This provides confidence that the models will be measuring the specific analyte and not inferring based on a correlation with another component. This is particularly important for ensuring models are robust as slight changes may result in the models no longer being able to perform effectively if they rely on correlations of other components. It is important to note that minimal differences were observed in the correlation matrices for

glucose concentration. This is likely due to variations in glucose feeds being built into the experiment that is, a DOE was performed to vary glucose set point in the vessels. As a result, correlations were already broken and therefore further spiking additions did not appear to improve this further. In addition, the correlation matrix showed little difference for lactate concentration. This may be due to the spiking solutions used being in the range already captured with the non-spiking samples. Further improvement in correlation and model performance may be sought using a larger range of spiked samples.

3.7 | Transfer of models developed using miniature bioreactor cultures to predict glucose concentration at 50 L SUB scale

Accurate OPLS models for glucose concentration in cell cultures were developed using Raman spectra generated with the integrated miniature bioreactor solution. Further analysis was then carried out to determine the potential of using spectral data acquired of cell culture in miniature bioreactors for on-line monitoring at 50 L scale.

A prototype of a 50 L SUB, containing an integrated optical window, was evaluated. For the 50 L SUB integrated setup, the spectral window was fully integrated to the SUB and gamma-irradiated prior to use. The Raman probe head was then attached to the outside of the bag removing the need for sterilizing an in-situ probe. The optical light path and window geometry and material was identical to the

TABLE 3 Correlation matrix of reference data without spiked samples

w/o spiking	Batch age (hr)	Glucose	Lactate	Glutamine	Glutamate	NH3	Product
Batch age (hr)	1	0.294	0.270	0.608	0.038	0.573	0.739
Glucose	0.294	1	0.072	−0.143	−0.455	−0.004	0.037
Lactate	0.270	0.072	1	0.012	0.033	0.143	0.143
Glutamine	0.608	−0.143	0.012	1	0.280	0.325	0.886
Glutamate	0.038	−0.455	0.033	0.280	1	−0.014	0.013
NH3	0.573	−0.004	0.143	0.325	−0.014	1	0.439
Product	0.739	0.037	0.143	0.886	0.013	0.439	1

Note: Strong correlation is identified by values above 0.6.

TABLE 4 Correlation matrix of reference including spiked samples

Spiking	Batch age (hr)	Glucose	Lactate	Glutamine	Glutamate	NH3	Product
Batch age (hr)	1	0.310	0.265	0.139	0.052	0.223	0.524
Glucose	0.310	1	0.073	−0.120	−0.294	−0.010	0.019
Lactate	0.265	0.073	1	−0.058	0.006	0.021	0.109
Glutamine	0.139	−0.120	−0.058	1	−0.022	−0.025	0.084
Glutamate	0.052	−0.294	0.006	−0.022	1	−0.090	−0.049
NH3	0.223	−0.010	0.021	−0.025	−0.090	1	0.119
Product	0.524	0.019	0.109	0.084	−0.049	0.119	1

Note: Strong correlation is identified by values above 0.6.

miniature bioreactor integrated solution allowing the same Raman probe head to be used at both scales, facilitating model transfer. The geometry also resulted in the sample channel exposed to the spectral window for Raman acquisition being enclosed, reducing light interference frequently experienced when using in-situ probes.²⁷ At present, it is common practice to cover large-scale vessels with aluminium foil to reduce interference from ambient light. This is not practical, especially at large scale and therefore the use of this prototype facilitates easier setup and operation of large scale SUB while resulting in better quality spectra. Upon completion of the run, the internal sample channel was assessed for clogging as a result of increased cell density (cell concentrations reached up to 31×10^6 cells/ml with 98% viability). No clogging was observed or spectral artefacts from bubbles were detected in the spectra, neither was any ambient light interference.

OPLS was used to develop a predictive model correlating glucose concentration with spectral data acquired during the three miniature bioreactor runs and spectral data acquired during the first 50 L SUB

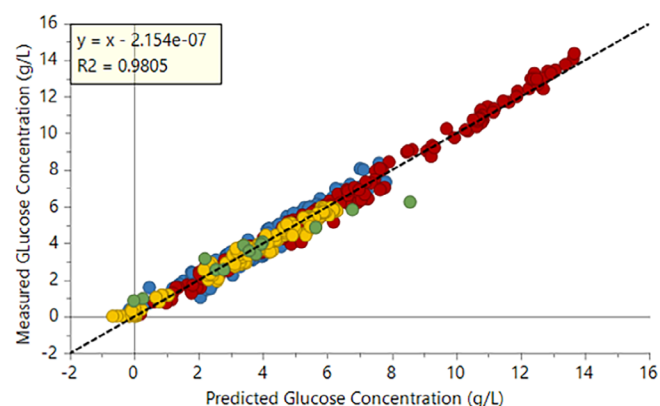
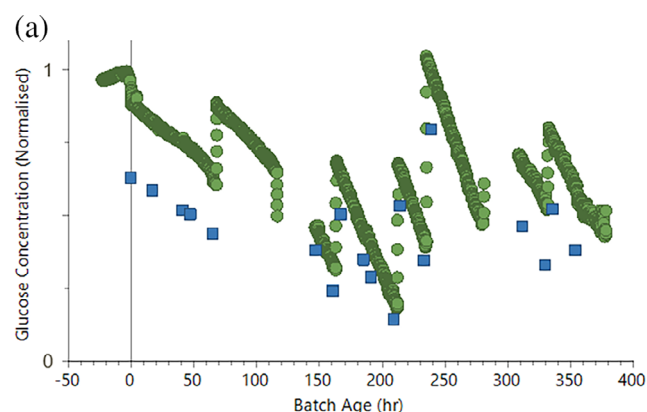


FIGURE 8 Observed versus predicted (cross-validation) plot for the OPLS model developed to predict glucose concentration using spectral data from; green: 50 L SUB (batch 1), blue: miniature bioreactor (run 1), red: miniature bioreactor (run 2), yellow: miniature bioreactor (run 3). OPLS, orthogonal-partial least squares



batch. Figure 8 displays the observed versus predicted plot of the OPLS model developed. The predictions using Raman spectra acquired of cell culture at the 50 L scale overlays well with the ambr[®]15 batches, however the CV error increases (0.67 g/L).

The OPLS model developed correlating glucose concentration with the three miniature bioreactor runs and the first 50 L SUB batch was then used to predict a separate 50 L SUB batch (Batch 3). Figure 9 displays the observed versus predicted over batch age (hr) before (A) and after (B) a one-point calibration.

Overall the prediction error was 1.89 g/L. Following a single-point calibration this further improved to 0.99 g/L RMSEP. These results are extremely promising, demonstrating the potential of transferring and using a model built on small scale data with a requirement of only using a single large scale batch followed by a single-point calibration. It was evident in this study that postbatch detected spectral variations in the sapphire window of the SUB and the ambr[®] flow cell likely had a significant impact on the offset observed. Improvement in window material is likely to achieve higher consistency between systems for improved model transfer. This evaluation demonstrates the potential of the integrated solution to facilitate model transfer across scales.

4 | CONCLUSION

Miniature bioreactors are increasingly being utilized in the biopharmaceutical industry for early cell line selection screening and process de-risking for larger scale. To facilitate technology continuity and model transfer, an integrated spectroscopy solution to both miniature bioreactor scale and large scale SUB was evaluated. It was demonstrated that accurate models could be developed using the integrated miniature bioreactor solution. Furthermore, it was shown that the addition of spiking known concentrations of analytes into cell culture samples prior to Raman acquisition can increase the range in concentration observed by the calibration models and break correlations between analytes, building robustness into model development. The development and use of the integrated solution at 50 L scale enabled on-line

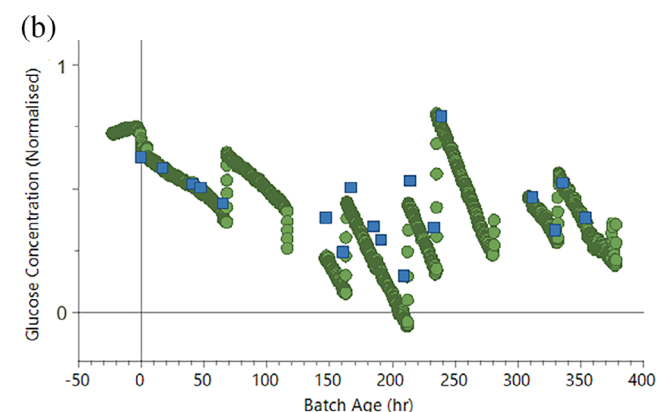


FIGURE 9 Time series of predicted (green) glucose concentration and observed (blue) glucose concentration of a model calibrated with $3 \times$ ambr[®]15 data and $1 \times$ SUB data and used to predict glucose concentration in a separate SUB run (a) prior to a one-point calibration (b) after a one-point calibration

monitoring at large scale without the need for sterilizing a traditional in-situ probe. Due to the design of the SUB integrated spectral window, minimal light interference was observed improving spectra generated in large-scale vessels. It was demonstrated that a predictive model for glucose concentration using spectral data acquired of cell culture at small scale could be used to accurately measure glucose concentration at 50 L scale. Utilizing data at small scale with experimental variations is important for robust model generation that would be very costly if not impossible to perform at larger scale. The implementation of this technology across scales will enable automated spectral acquisition at small scale, technology, and operation continuity across scales and facilitate model transfer from development through to commercialization.

ACKNOWLEDGMENTS

We would like to thank Alex Livingstone (GSK) who operated the 50 L SUB. Thank you also to James Roberts (Bachelors student at Leeds University) who performed some initial trouble shooting work in the very early stages of the study and to Sophie James (Bachelors student at York University) who assisted in the running of the ambr[®]15 miniature bioreactors.

PEER REVIEW

The peer review history for this article is available at <https://publons.com/publon/10.1002/btpr.3074>.

ORCID

Ruth C. Rowland-Jones  <https://orcid.org/0000-0002-3678-2791>

Alexander Graf  <https://orcid.org/0000-0002-0401-7470>

Paloma Diaz-Fernandez  <https://orcid.org/0000-0002-4299-3667>

REFERENCES

- Mordor Intelligence LLP. Biopharmaceuticals Market - Growth, Trends, and Forecast (2019–2024), 2019.
- Lalor F, Fitzpatrick J, Sage C, Byrne E. Sustainability in the biopharmaceutical industry: seeking a holistic perspective. *Biotechnol Adv.* 2019;37(5):698–707. <https://doi.org/10.1016/j.biotechadv.2019.03.015>.
- Shanmugaraj B, Siri Wattananon K, Wangkanont K, Phoolcharoen W. Perspectives on monoclonal antibody therapy as potential therapeutic intervention for coronavirus disease-19 (COVID-19). *Asian Pac J Allergy Immunol.* 2020;38(1):10–18. <https://doi.org/10.12932/AP-200220-0773>.
- Mora A, Zhang SS, Carson G, Nabiswa B, Hossler P, Yoon S. Sustaining an efficient and effective CHO cell line development platform by incorporation of 24-deep well plate screening and multivariate analysis. *Biotechnol Prog.* 2018;34(1):175–186. <https://doi.org/10.1002/btpr.2584>.
- Sokolov M, Morbidelli M, Butté A, Souquet J, Broly H. Sequential multivariate cell culture modeling at multiple scales supports systematic shaping of a monoclonal antibody toward a quality target. *Biotechnol J.* 2018;13(4):e1700461. <https://doi.org/10.1002/biot.201700461>.
- Kreye S, Stahn R, Nawrath K, Goralczyk V, Zoro B, Goletz S. A novel scale-down mimic of perfusion cell culture using sedimentation in an automated microbioreactor (SAM). *Biotechnol Prog.* 2019;35(5):e2832. <https://doi.org/10.1002/btpr.2832>.
- Zhang X, Moroney J, Hoshan L, Jiang R, Xu S. Systematic evaluation of high-throughput scale-down models for single-use bioreactors (SUB) using volumetric gas flow rate as the criterion. *Biochem Eng J.* 2019;151:107307. <https://doi.org/10.1016/j.bej.2019.107307>.
- U.S. Department of Health and Human Services. PAT - A Framework for Innovative Pharmaceutical Development, Manufacturing, and quality assurance. 1, 2004.
- Berry BN, Dobrowsky TM, Timson RC, Kshirsagar R, Ryll T, Wiltberger K. Quick generation of Raman spectroscopy based in-process glucose control to influence biopharmaceutical protein product quality during mammalian cell culture. *Biotechnol Prog.* 2016;32(1):224–234. <https://doi.org/10.1002/btpr.2205>.
- Matthews TE, Berry BN, Smelko J, Moretto J, Moore B, Wiltberger K. Closed loop control of lactate concentration in mammalian cell culture by Raman spectroscopy leads to improved cell density, viability, and biopharmaceutical protein production. *Biotechnol Bioeng.* 2016;113(11):2416–2424. <https://doi.org/10.1002/bit.26018>.
- Powers DN, Wang Y, Fratz-Berilla EJ, et al. Real-time quantification and supplementation of bioreactor amino acids to prolong culture time and maintain antibody product quality. *Biotechnol Prog.* 2019;35(6):e2894. <https://doi.org/10.1002/btpr.2894>.
- Zavala-Ortiz DA, Ebel B, Li M-Y, et al. Interest of locally weighted regression to overcome nonlinear effects during in situ NIR monitoring of CHO cell culture parameters and antibody glycosylation. *Biotechnol Prog.* 2020;36(1):e2924. <https://doi.org/10.1002/btpr.2924>.
- Rowland-Jones RC, Jaques C. At-line Raman spectroscopy and design of experiments for robust monitoring and control of miniature bioreactor cultures. *Biotechnol Prog.* 2019;35(2):e2740. <https://doi.org/10.1002/btpr.2740>.
- Ryder AG, Vincentis JD, Li B, Ryan PW, Sirimuthu NMS, Leister KJ. A stainless steel multi-well plate (SS-MWP) for high-throughput Raman analysis of dilute solutions. *J Raman Spectrosc.* 2010;41(10):1266–1275. <https://doi.org/10.1002/jrs.2586>.
- Musmann C, Joeris K, Markert S, Solle D, Scheper T. Spectroscopic methods and their applicability for high-throughput characterization of mammalian cell cultures in automated cell culture systems. *Eng Life Sci.* 2016;16(5):405–416. <https://doi.org/10.1002/elsc.201500122>.
- Berry B, Moretto J, Matthews T, Smelko J, Wiltberger K. Cross-scale predictive modeling of CHO cell culture growth and metabolites using Raman spectroscopy and multivariate analysis. *Biotechnol Prog.* 2015;31(2):566–577. <https://doi.org/10.1002/btpr.2035>.
- Webster TA, Hadley BC, Hilliard W, Jaques C, Mason C. Development of generic Raman models for a GS-KOTM CHO platform process. *Biotechnol Prog.* 2018;34(3):730–737. <https://doi.org/10.1002/btpr.2633>.
- Brouckaert D, Uyttensprot J-S, Broeckx W, Beer T d. Calibration transfer of a Raman spectroscopic quantification method from at-line to in-line assessment of liquid detergent compositions. *Anal Chim Acta.* 2017;971:14–25. <https://doi.org/10.1016/j.jaca.2017.03.049>.
- Goldrick S, Sandner V, Cheeks M, et al. Multivariate data analysis methodology to solve data challenges related to scale-up model validation and missing data on a micro-bioreactor system. *Biotechnol J.* 2020;15(3):e1800684. <https://doi.org/10.1002/biot.201800684>.
- Eilers, P. H.C.; Boelens, H. F.M. Baseline correction with asymmetric least squares smoothing, 2005.
- Eriksson L, Byrne T, Johansson E, Trygg J, Vikström C. *Multi- and Megavariate Data Analysis. Basic Principles And Applications, Third Revised Edition; Umetrics Academy - Training in Multivariate Technology.* Umeå: Umetrics; 2013.
- Rowland-Jones RC, van den Berg F, Racher AJ, Martin EB, Jaques C. Comparison of spectroscopy technologies for improved monitoring of cell culture processes in miniature bioreactors. *Biotechnol Prog.* 2017;33(2):337–346. <https://doi.org/10.1002/btpr.2459>.
- Abu-Absi NR, Kenty BM, Cuellar ME, et al. Real time monitoring of multiple parameters in mammalian cell culture bioreactors using an

- in-line Raman spectroscopy probe. *Biotechnol Bioeng*. 2011;108(5): 1215-1221. <https://doi.org/10.1002/bit.23023>.
24. Monod J. The growth of bacterial cultures. *Annu Rev Microbiol*. 1949;3 (1):371-394. <https://doi.org/10.1146/annurev.mi.03.100149.002103>.
25. Dumont J, Euwart D, Mei B, Estes S, Kshirsagar R. Human cell lines for biopharmaceutical manufacturing: history, status, and future perspectives. *Crit Rev Biotechnol*. 2016;36(6):1110-1122. <https://doi.org/10.3109/07388551.2015.1084266>.
26. López-Meza J, Araíz-Hernández D, Carrillo-Cocom LM, López-Pacheco F, Rocha-Pizaña MDR, Alvarez MM. Using simple models to describe the kinetics of growth, glucose consumption, and monoclonal antibody formation in naive and infliximab producer CHO cells. *Cytotechnology*. 2016;68(4):1287-1300. <https://doi.org/10.1007/s10616-015-9889-2>.
27. Sowoidnich K, Towrie M, Matousek P. Lock-in detection in Raman spectroscopy with charge-shifting CCD for suppression of fast varying backgrounds. *J. Raman Spectrosc*. 2019;49:983-995. <https://doi.org/10.1002/jrs.5597>.

How to cite this article: Rowland-Jones RC, Graf A, Woodhams A, et al. Spectroscopy integration to miniature bioreactors and large scale production bioreactors–Increasing current capabilities and model transfer. *Biotechnol Progress*. 2020;e3074. <https://doi.org/10.1002/btpr.3074>